



SEISMIC FRAGILITY ANALYSIS WITH RANDOM IDA METHOD UNDER DIFFERENT SEISMIC FORTIFICATION LEVELS

B. JIN⁽¹⁾, Z.R. FENG⁽¹⁾, Z.W. LI⁽²⁾, Y.Y. NIU⁽¹⁾, Y. BAI⁽³⁾

⁽¹⁾ Associate professor, Key Laboratory of Earthquake Engineering and Engineering Vibration of CEA, Institute of Engineering Mechanics, China Earthquake Administration (CEA) Harbin, Heilongjiang, 150080, China, jinbo@iem.ac.cn

⁽²⁾ Senior engineer, Jilin Earthquake Agency Changchun, Jilin, 132000, China, 858793951@qq.com

⁽³⁾ Engineer, Seismological Bureau of Qianguoerros Mongolian Autonomous County, Songyuan, Jilin, 131100, China, 1084492670@qq.com

Abstract

In fact, increasing collapse resistance is the most important objective of performance-based aseismic design. In this paper, at first, a five-storey and three-bay RC frame structure model with different seismic fortification levels is established by OpenSEES. Based on the corresponding principle, several appropriate ground motions have been selected as input. Meanwhile, considering the uncertainty of both ground motions and structural design parameters, a series of corresponding seismic structure models are matched by LHS (Latin hypercube sampling) method. Then the maximum inter-story displacement is selected as the response index of nonlinear time history analysis of the structure models, and the vulnerability curves of the structure models with different seismic fortification levels are established, in which the PGA and the structural failure probability are taken as x coordinates and y coordinates respectively. Finally, the necessity of improving the seismic fortification design and construction of key fortification buildings in current design codes is verified by the series of seismic fragility analyses.

Seismic fortification is one of the core contents of the current Chinese national seismic code. In the 3-level defense requirements for seismic design of the national code, the third one, guarantee collapse resistance to big earthquakes is the most important objective of performance-based aseismic design. However, because of the complexity of aseismic structure and the randomness of earthquake ground motions, the third level proposal is merely based on engineering experience, conceptual design and constructional measures. In this paper, the uncertainty of both ground motions and structural design parameters are considered together. Through a series of seismic fragility analyses to an actual RC frame structure, the necessity and the theoretical property of the third level to seismic fortification design is verified by numerical analyzing. It will provide reference and way for calculation and quantitative analysis of seismic fortification levels for implementation in the future.

Keywords: fragility analysis; IDA; LHS; RC frame; seismic fortification



1. Introduction

Performance-based seismic design (PBSD) is that according to the importance and the design purpose of buildings, different performance levels and applications will be divided separately, from which different seismic fortification criteria are derived, then to make designed structures satisfy the respected performance requirements under the action of various possible earthquakes [1]. The classification of theoretical analysis and calculation methods for structural seismic vulnerability can be divided into "direct method" and "indirect method". The direct method can be understood as a Monte Carlo simulation method. The direct method is to replace the seismic survey data in empirical vulnerability analysis with finite element analysis data. By comparing the results of finite element analysis with the definitions of failure state, the probability of structural damage under different earthquake intensity can be obtained. Then, according to the probability of structural damage, the seismic vulnerability curve can be further fitted or the failure probability matrix can be generated. Singhal and Kiremidjian[2] obtained seismic vulnerability curve and failure probability matrix of reinforced concrete frame structures based on damage index by the direct method. Professor Elnashai and his collaborators used direct methods to analyze seismic vulnerability of bridge structures[3], flat-slab structures[4], and high-rise concrete structures[5]. Chinese scholar Liu Jingbo cooperated with H Hwang[6, 7], and made an in-depth research on seismic vulnerability of reinforced concrete bridge structures in Central America by the direct method. Zhu Jian[8] also used the direct method to analyze seismic vulnerability of reinforced concrete structures.

Comparing with the direct method of obtaining the failure probability of structures under earthquake action, the indirect method of seismic vulnerability converts the study of seismic vulnerability into a classical reliability problem: $F(x) = P[S > R / IM = x]$.

Where, R and S are the resistance and reaction of the structure, respectively, and $F(x)$ is the vulnerability of the structure. On the premise that both R and S obey lognormal distribution, the seismic vulnerability function $F(x)$ can be expressed as follows:

$$F(x) = \Phi\left[\frac{\ln m_S - \ln m_R}{\sqrt{\beta_S^2 + \beta_R^2}}\right] \quad (1)$$

In which, m_S , m_R , β_S and β_R are respectively the median and logarithmic standard deviations of structural response and resistance.

According to the equation(1), seismic vulnerability analysis is divided into two parts: probabilistic seismic demand analysis and probabilistic seismic capacity analysis. These two parts correspond to the probabilistic seismic demand model and the probabilistic seismic capacity model in the performance-based earthquake engineering (PBEE) probabilistic decision framework proposed by PEER. Using the indirect method, Professor Ellingwood and his collaborators have done much research on seismic vulnerability of steel frame [9], concrete frame [10] and wood structure [11]. Dimova and Negrone [12] have carried out seismic vulnerability analysis of building structures designed in accordance with European codes. Professor LvDagang and his collaborators have studied seismic vulnerability of steel frame structures [13], reinforced concrete frame structures [14-16] and concrete continuous girder bridges [17].

2 Selection of Uncertainty Parameters and Structural Design

In this paper, three typical three-span and five-story frame structures are built by OpenSEES according to 7-degree, 8-degree and 9-degree fortifications respectively. All the proposed sites are classified as class II, and the design earthquakes are grouped into group II.

2.1 Structural Layout, Section Size and Reinforcement



The layout of the structure is shown in Fig. 1. It is a typical inner corridor layout, which is common to schools and hospitals. The elevation of the structure is shown in Fig. 2.

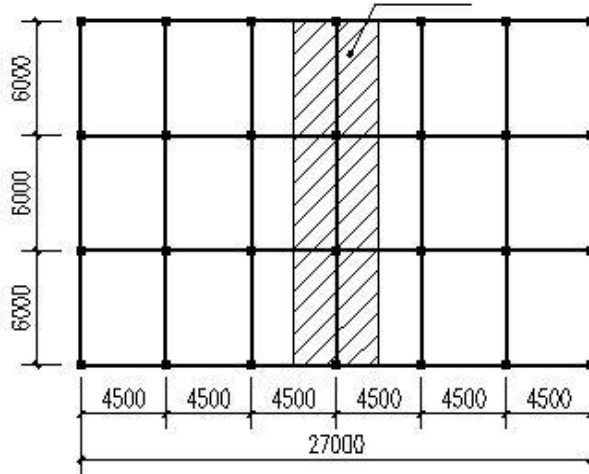


Fig. 1 – Plan and Elevation of RC frame

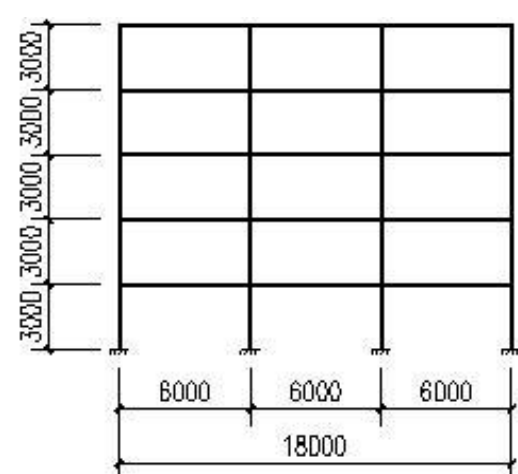


Fig. 2 – Elevation of RC frame

The intermediate frame (shadow part in Fig. 1) is designed, modelled and analyzed respectively. The non-linear analysis model of plane frame structure is established by OpenSEES software. The displacement-based non-linear beam-column element is used for beam and column members, and the fibre section model is used for beam-column section. Concrete 02 is used for concrete constitutive model. The model skeleton curve is Kent-Park model expanded by Scott et al.[21][22] The model considers the restraint effect of transverse stirrups by modifying the peak stress, strain of unconstrained concrete compressive skeleton curve and the slope of softening section. Steel 02 is a constitutive model proposed by Menegotto and Pugno and modified by Filippou et al., in which consider the effect of isotropic strain hardening and the Bauschinger effect.

According to the current code for seismic design of buildings in China [24], the internal force analysis, load combination and section reinforcement are carried out by using the PKPM software. The section size of beams and columns designed in this example is mainly controlled by the maximum inter-story displacement angle under small earthquakes. The specific section size and parameters are shown in Table 1.

Table 1 – Cross-section sizes and reinforcement in beams and columns

SI	7-Degree, 3 Level		8-Degree, 2 Level		9-Degree, 1 Level	
	LR	Stirrups,0.75%	LR	Stirrups,0.89%	LR	Stirrups,1.09%
	450 × 450(mm),LR ρ =0.7%		550 × 600(mm),LR ρ =0.8%		600 × 800(mm),LR ρ =0.9%	
C	1417.5	3φ8@200	2640	3φ10@200	4800	4φ10@200
	4φ14	3φ8@100	4φ20	3φ10@100	8φ22	4φ10@100
	4φ16		4φ22		4φ25	
	App.1419	0.77%	App.2776	0.92%	App.5005	1.10%
	260 × 500(mm),LR ρ =0.26%		300 × 600(mm),LR ρ =0.31%		350 × 800(mm),LR ρ =0.4%	
B	229	2φ8@200	521	2φ10@200	1120	3φ10@200



	4φ12	2φ8@100	4φ14	2φ10@100	6φ16	3φ10@100
	App.452	0.95%	App.615	1.00%	App.1206	1.02%

(Note:LR --Longitudinal reinforcement, SI—Seismic intensity, C—Column, B—Beam)

2.2 Selection of Structural Uncertainty Parameters

In addition to being closely related to the input earthquake motions, the seismic capacity of the structure is also affected by many structural uncertainties. Structural uncertain factors mainly refer to various uncertainties in building structural models, including uncertainties in material properties, geometric parameters of components, restoring force model and mechanical model.

In this paper, concrete02 in OpenSEES material library is used to build the model. According to the calculation formula model of Kent-Park and the different reinforcement ratios under the 7-degree, 8-degree and 9-degree fortifications, the strength enhancement coefficients K of concrete under three fortification intensities are calculated respectively, considered the confinement of stirrups. For the uncertainties of reinforced concrete frame structures in this paper, ten structural uncertainties, including damping and structural materials, are considered as shown in Table 2.

Table 2 – Structural random parameters

Uncertainty	Random variable	7-degree fortification	8-degree fortification	9-degree fortification	CV	Distribution pattern
Concrete C30	f_{co}	26.1MPa			0.14	Log-Normal
	$f_{cc,beam}$	28.95MPa	29.10MPa	29.16MPa	0.21	
	$\varepsilon_{cc,beam}$	0.0022	0.0023	0.00223	0.17	
	$\varepsilon_{cu,beam}$	0.0126	0.0130	0.0132	0.52	
	$f_{cc,column}$	28.41MPa	28.86MPa	29.13MPa	0.21	
	$\varepsilon_{cc,column}$	0.0022	0.0022	0.0022	0.17	
	$\varepsilon_{cu,column}$	0.0109	0.0123	0.0131	0.52	
Rebar HRB335	f_y	378MPa			0.07	Log-Normal
	E_s	2×10^5 MPa			0.02	
VDR	$\varepsilon_{cp,cov er}$	0.65			0.4	Normal

(Note: CV—Coefficient of variation, VDR—Viscous damping ration)

In the Table 2, f_{co} is the peak stress of enclosed unconstrained concrete, and $f_{cc,beam}$ is the peak stress of restrained concrete beam, and $\varepsilon_{cc,beam}$ is the peak strain of restrained concrete beam, and $\varepsilon_{cu,beam}$ is the limit strain of restrained concrete beam, and $f_{cc,column}$ is the peak stress of restrained concrete column, and $\varepsilon_{cc,column}$ is the peak strain of restrained concrete column, and $\varepsilon_{cu,column}$ is the limit strain of restrained



concrete column, and f_y is the yield strength of steel bar, and E_s is the elastic modulus of steel bar, and ζ is the structural viscous damping coefficient.

3. Uncertainty of Earthquake motion and Selection of Seismic Waves

3.1 Wave Selection Principle of Earthquake

Because earthquake motion is a non-stationary stochastic process with a wide frequency band, it is highly uncertain due to the influence of earthquake generating mechanism, propagation medium and site condition. Therefore, it is particularly important to select earthquake motion reasonably in IDA analysis. The US ATC-63 (2008) report [18] recommended 22 far-field seismic waves and 28 near-field seismic waves.

3.2 Selection of Earthquake Motion

The 15 earthquake motion records are selected from the earthquake motion database as shown in Table 3.

Table 3 – Earthquake motion records

No.	Earthquake motion	Year	Location	Component	PGA(g)
1	Chi-Chi,Taiwan	1999	CHY101	CHY101-N	0.440
2	Northridge	1994	Beverly Hills-Mulhol	MUL279	0.516
3	Imperlay valley	1981	El Centro Array #11	HE11230	0.380
4	Friuli,Italy	1976	8014 ForgariaCornino	B-FOC000	0.260
5	Superstition Hills	1981	Poe Road	B-POE360	0.300
6	Kocaeli,Turkey	1999	Duzce	DZC270	0.358
7	Morgan Hill	1984	Gilroy Array #3	G03-UP	0.395
8	Loma Prieta	1989	Gilroy Array #3	GO30090	0.200
9	Superstition Hills	1987	EI Centro Imp.Co.Cent	ICC090	0.258
10	Westmorland	1981	Westmorland Fire	WSM090	0.368
11	Imperial Valley	1940	117 El Centro Array #9	I-ELC270	0.215
12	Landers	1992	Yermo Fire Station	YER270	0.245
13	Loma Prieta	1989	57382 Gilroy Array #4	G04090	0.212
14	Northridge	1994	LA - Hollywood Stor FF	HOL360	0.358
15	San Fernando	1971	LA - Hollywood Stor Lot	PEL090	0.210

4. Nonlinear dynamic time history analysis based on stochastic IDA method

4.1 Latin Hypercube Sampling

The basic principles of Latin hypercube sampling are as follows. Firstly, in the extraction of random variable samples, the complete random selection in the past is changed to the average selection in the equal probability interval. Secondly, in the combination of random samples, the random collocation method is adopted. Zhang Lingxin and Jiang Jinren used Latin hypercube sampling to calculate the reliability of the



structure, which greatly reduced the number of samples [19]. Latin hypercube sampling method can effectively distribute the samples uniformly in all range of random variables, so it is much more efficient than Monte Carlo method which only uses random sampling.

4.2 Random Matching for 15 Motion-Structure Model Sets of Earthquakes

Using the Latin hypercube sampling method and MATLAB, 15 groups of earthquake motions and 9 uncertain structural parameters are randomly sampled and matched to 15 groups of earthquake motions-structure model sets, as shown in Table 4.

Table 4 – Motion-structure model set of earthquake under different seismic fortification levels

(a) Motion-structure model set of earthquake under 7-degree fortification level										
	f_y	E_s	f_{co}	$f_{cc,column}$	$\varepsilon_{cc,column}$	$\varepsilon_{cu,column}$	$f_{cc,beam}$	$\varepsilon_{cc,beam}$	$\varepsilon_{cu,beam}$	GMX
1	366.29	205507	25.41	38.65	0.00154	0.01087	21.49	0.00230	0.01409	11
2	412.70	203534	21.25	26.28	0.00233	0.01078	24.56	0.00189	0.01213	10
3	404.12	206175	16.54	30.92	0.00208	0.01003	27.92	0.00178	0.01033	4
4	392.01	204739	30.22	23.86	0.00267	0.01175	34.45	0.00205	0.01316	13
5	374.32	202448	23.17	25.40	0.00213	0.01149	33.93	0.00247	0.01583	3
6	401.11	203310	28.02	26.89	0.00197	0.01239	29.36	0.00218	0.01099	6
7	368.85	204309	28.90	19.37	0.00238	0.01252	22.99	0.00196	0.01288	5
8	386.27	204907	27.35	28.74	0.00226	0.01036	31.09	0.00251	0.01346	1
9	435.16	201880	32.05	30.27	0.00222	0.00899	29.32	0.00211	0.01124	12
10	344.31	201062	35.42	27.69	0.00201	0.01118	27.54	0.00261	0.01361	2
11	378.34	203892	23.90	34.45	0.00246	0.00755	32.32	0.00239	0.01500	9
12	349.69	202827	20.33	22.73	0.00256	0.01385	26.49	0.00228	0.01246	8
13	355.75	206552	26.88	31.44	0.00185	0.00974	25.11	0.00274	0.00790	7
14	424.71	198461	24.43	29.02	0.00176	0.00959	38.35	0.00221	0.01229	14
15	387.07	209069	26.28	32.77	0.00219	0.01193	30.15	0.00126	0.01181	15

(b) Motion-structure model set of earthquake under 8-degree fortification level										
	f_y	E_s	f_{co}	$f_{cc,column}$	$\varepsilon_{cc,column}$	$\varepsilon_{cu,column}$	$f_{cc,beam}$	$\varepsilon_{cc,beam}$	$\varepsilon_{cu,beam}$	GMX
1	387.54	204538	30.16	35.87	0.00194	0.01395	31.03	0.00240	0.01273	11
2	399.73	202595	33.98	20.63	0.00201	0.01142	28.71	0.00201	0.01216	10
3	375.60	202747	28.88	24.84	0.00265	0.01190	23.07	0.00229	0.01179	4
4	381.55	203148	24.96	27.42	0.00203	0.01167	25.63	0.00236	0.01431	13
5	440.69	203665	22.54	29.39	0.00252	0.01000	27.48	0.00154	0.01389	3



6	395.93	204915	15.21	27.98	0.00219	0.01276	30.10	0.00266	0.01864	6
7	423.78	206154	26.75	33.28	0.00210	0.01512	34.77	0.00216	0.01292	5
8	369.81	201615	19.86	25.97	0.00242	0.01434	33.97	0.00210	0.01317	1
9	339.58	200608	26.09	26.13	0.00270	0.01227	31.52	0.00207	0.01447	12
10	346.93	205333	28.29	35.47	0.00177	0.01089	15.96	0.00279	0.01229	2
11	407.67	208082	27.97	23.19	0.00215	0.01345	36.54	0.00253	0.01511	9
12	366.60	206629	25.67	28.76	0.00144	0.00984	32.72	0.00194	0.00982	8
13	358.74	204507	21.24	31.92	0.00232	0.01117	24.56	0.00186	0.01354	7
14	384.71	202106	23.97	30.37	0.00226	0.01326	28.04	0.00222	0.01099	14
15	406.86	204102	31.42	31.27	0.00238	0.01248	26.52	0.00247	0.01142	15

(c) Motion-structure model set of earthquake under 9-degree fortification level

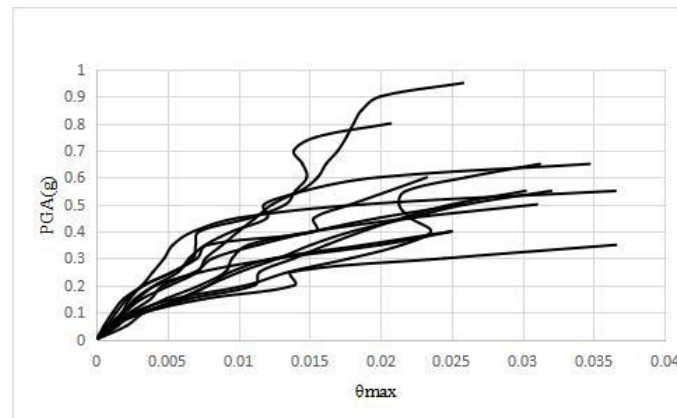
	f_y	E_s	f_{co}	$f_{cc,column}$	$\varepsilon_{cc,column}$	$\varepsilon_{cu,column}$	$f_{cc,beam}$	$\varepsilon_{cc,beam}$	$\varepsilon_{cu,beam}$	GMX
1	331.14	208484	27.89	29.34	0.00190	0.01577	31.32	0.00218	0.01030	11
2	368.83	203812	18.19	20.90	0.00218	0.01204	29.83	0.00221	0.01102	10
3	436.45	203941	26.42	26.16	0.00268	0.01048	28.02	0.00189	0.01148	4
4	363.77	204402	20.73	27.61	0.00298	0.01361	35.18	0.00277	0.01334	13
5	344.97	206568	22.95	27.96	0.00251	0.01135	25.59	0.00206	0.01385	3
6	422.11	205637	25.59	24.12	0.00179	0.01393	18.59	0.00198	0.01285	6
7	388.15	203034	28.76	27.00	0.00168	0.01432	33.32	0.00239	0.01447	5
8	398.63	199338	29.83	30.70	0.00207	0.01285	27.07	0.00138	0.01680	1
9	360.06	206181	26.47	39.91	0.00212	0.01056	29.30	0.00234	0.01395	12
10	379.63	205267	30.85	22.60	0.00244	0.01319	24.61	0.00230	0.01467	2
11	412.61	203310	24.68	33.70	0.00242	0.01476	40.92	0.00255	0.01261	9
12	393.48	204836	24.18	35.34	0.00221	0.01552	30.43	0.00243	0.01318	8
13	405.50	201452	31.84	31.16	0.00198	0.01180	23.59	0.00210	0.01565	7
14	376.59	202357	21.78	30.00	0.00226	0.01249	27.76	0.00267	0.01204	14
15	384.54	201856	35.95	32.38	0.00232	0.01325	32.62	0.00196	0.01236	15

4.3 Analysis and Calculation of IDA Curve by Random IDA Method

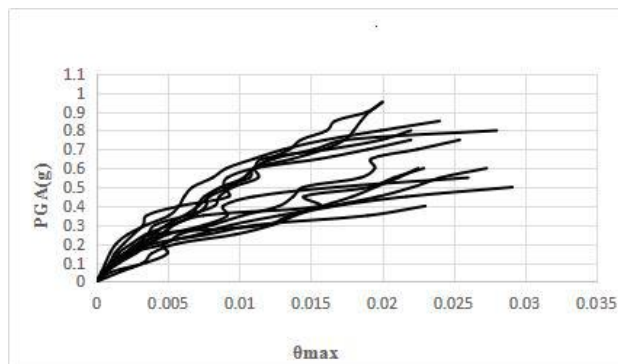


The basic method of Incremental Dynamic Analysis is to apply a seismic record to the structure, adjusting the seismic record to multiple intensity levels according to a certain proportion coefficient, and carrying out time history analysis at each intensity level to obtain a relationship curve between engineering demand parameters and seismic intensity index, namely IDA curve. Several IDA curves are obtained by changing earthquake motion records, and statistical analysis is carried out to evaluate the structural performance at different seismic levels.

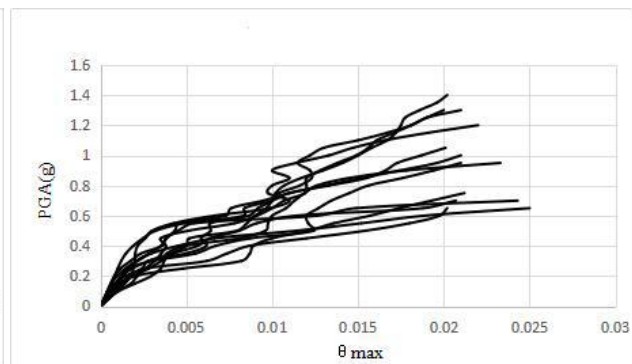
The stochastic IDA method is based on the IDA method, which considers both the earthquake motion and the structural uncertainty. According to the random matched motion-structure model set of earthquake under 7-degree fortification, 8-degree fortification and 9-degree fortification, the corresponding IDA curves are obtained by the non-linear dynamic time history analysis respectively, as shown in Fig. 3.



(a) IDA curve under 7-degree fortification



(b) IDA curve under 8-degree fortification



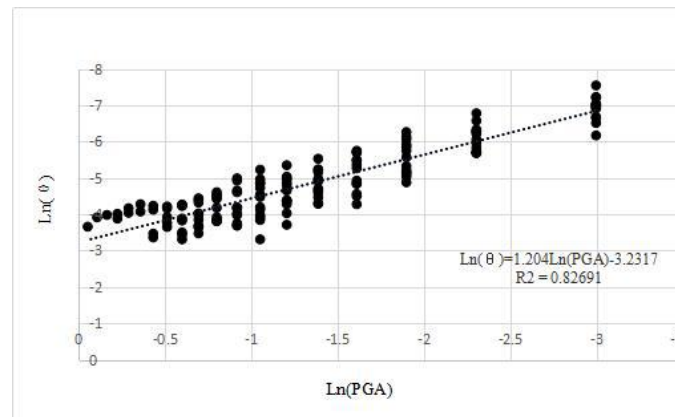
(c) IDA curve under 9-degree fortification

Fig. 3 – IDA curves under different fortification levels

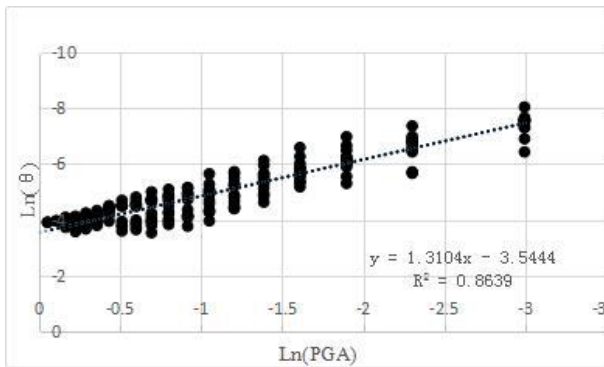
5. Regression analysis and vulnerability curves

5.1 Regression Analysis

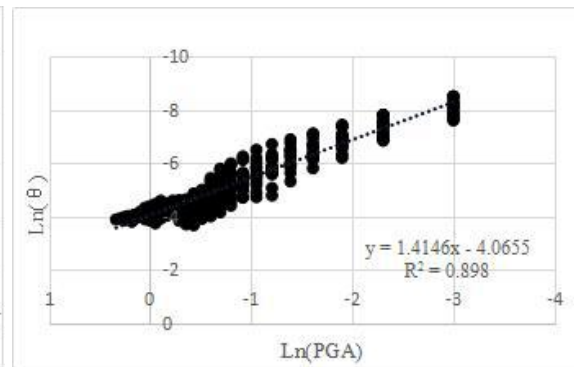
Regression analysis is made on the data obtained from the nonlinear dynamic time history analysis of stochastic IDA method. It is assumed that the peak acceleration PGA and the maximum inter-story displacement angle θ_{\max} of the structure abide by lognormal distribution. The natural logarithmic value of PGA, which is used to measure the intensity of earthquake motion, is taken as independent variable, and the natural logarithmic value of the maximum inter-story displacement angle θ_{\max} which represents the degree of structural damage is taken as dependent variable, and the regression analysis is shown as Fig. 4.



(a) Regression analysis under 7-degree fortification



(b) Regression analysis under 8-degree fortification



(c) Regression analysis under 9-degree fortification

Fig. 4 – Regression analysis under different fortification levels

5.2 Vulnerability Curve

According to the linear function between the natural logarithm of the peak acceleration PGA and the natural logarithm of the maximum interlayer displacement angle θ_{\max} obtained by the above regression analysis, $\text{Ln}(\theta_{\max}) = a \text{Ln}(PGA) + b$ is substituted into Equation(1).

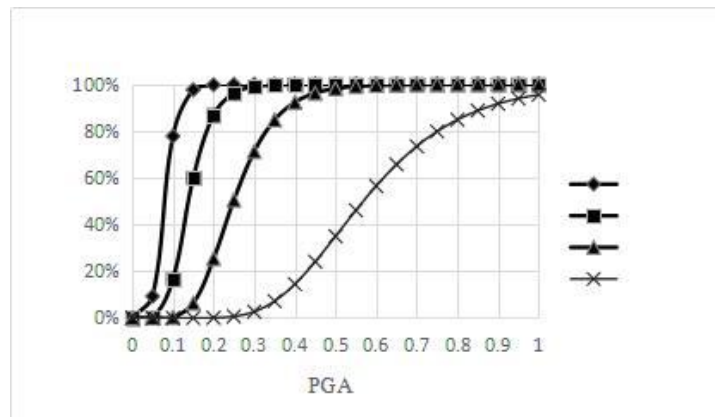
$$F(x) = \Phi\left[\frac{a \ln(PGA) + b - \ln m_R}{\sqrt{\beta_s^2 + \beta_R^2}}\right] \quad (2)$$

In which, $\sqrt{\beta_s^2 + \beta_R^2}$ is 0.4, and the limit value of structural capability parameter m_R in different limit states is shown in Table 5.

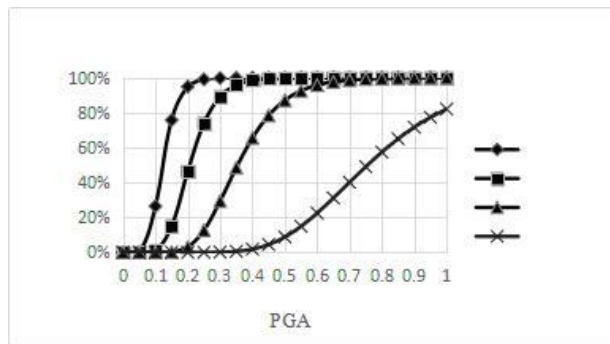
Table 5 – Limit value of different structural damage degree

Inter-story displacement	~1/550	1/550~1/275	1/275~1/135	1/135~1/50	1/50~
Damage	Basic integrity	Slight damage	Moderate	Serious	Collapse

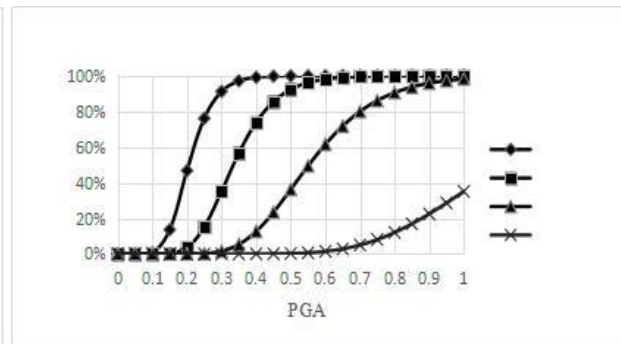
$\Phi(x)$ is a normal distribution function, and according to Equation(2), the failure probability of the structure represented by maximum peak acceleration PGA at 7, 8 and 9 degrees of fortification can be obtained, and then the vulnerability curve can be obtained, as shown in Fig. 5.



(a) Fragility curves under 7-degree fortification



(b) Fragility curves under 8-degree fortification



(c) Fragility curves under 9-degree fortification

Fig. 5 – Fragility curves under different fortification levels

The maximum acceleration time history for analysis of different fortification intensities are given by current seismic codes in China (as shown in Table 6). Considering the possibility of encountering a "mega-earthquake", the corresponding maximum acceleration time history for different fortification intensities under "mega-earthquake" is added [20].

Table 6 – The peak acceleration for time history analysis

Fortification intensity	PGA/gal	7	8	9
Weak Frequently		35	70	140
Frequent Earthquake		100	200	400
Rare Earthquake		220	400	620
Mega Earthquake		400	620	800

According to the maximum value of acceleration time history and vulnerability curve function under different seismic levels, the probability of different damage degree corresponding to different seismic levels under different seismic fortification intensity can be obtained as shown in Table 7.

Table 7 – Structural failure probability under different seismic fortification levels

Fortification intensity	PGA/gal	Different Probability	7	8	9
Weak Frequently		Slight Damage	0.97%	4.15%	8.97%
Rare Earthquake		Serious Damage	37.7%	67.9%	68.44%



	Collapse	0.26%	2.18%	2.26%
Mega Earthquake	Serious Damage	93%	97.1%	91.62%
	Collapse	15.92%	27.6%	13.5%

6. Conclusion

(1) RC frame structures with 7-degree seismic fortification, 8-degree seismic fortification and 9-degree seismic fortification were subject to earthquakes with corresponding seismic fortification intensity, and the probability of minor damage was 0.97%, 4.15% and 8.97% respectively, and the probability of collapse was 0.26%, 2.18% and 2.26% respectively. According to the recommendation of the ATC-63 report [23], "It is considered to meet the requirement of the large earthquake performance if the collapse probability of fortification under large earthquake is less than 10%." It can be seen that RC frame structures under different seismic fortification intensities designed in accordance with the current seismic code all meet the seismic fortification objectives of "small earthquake is not bad" and "large earthquake does not fall" [24].

(2) It can be seen that although the probability of collapse of RC frame structures with one-degree fortification improvement was only slightly reduced, the probability of severe damage was greatly reduced. There are also many non-structural components in the medical building, such as surgical equipment, oxygen pipes, medicine storage cabinets, etc. Severe damage to the structure will cause damage to the non-structural components, causing huge economic losses and also greatly affecting the normal operation of the hospital [25]. Therefore, it is also verified that the special fortification buildings and key fortification buildings specified in the code should strengthen their seismic measures according to the requirement that the seismic fortification intensity is one degree higher than the region area, which has a strong practical significance.

(3) When suffering a great earthquake, the collapse probabilities of the RC frame structure with the fortification intensity of 7, 8 and 9 degree are 15.92%, 27.6% and 13.5%, respectively. As we can see, the probability of collapse is greater than 10%, which does not achieve the third seismic fortification goal, which is guarantee collapse resistance to big earthquakes. In the meantime, the severe damage probability was greater than 90%, which was consistent with the phenomenon that the frame structures designed and constructed according to the corresponding fortification intensity in Wenchuan earthquake were severely damaged and had a high probability of collapse. It is shown that the structural safety reserve coefficient of RC frame structures designed and constructed according to the current seismic code is limited.

7. Acknowledgements

This work is partially supported by the Science Foundation of Institute of Engineering Mechanics, CEA (No. 2019C08), the Natural Science Foundation of Heilongjiang Province (No.LH2019E096), and the Three-in-one project of monitoring, prediction and research of CEA (Grant No. 3JH-201902021).

8. Copyrights

17WCEE-IAEE 2020 reserves the copyright for the published proceedings. Authors will have the right to use content of the published paper in part or in full for their own work. Authors who use previously published data and illustrations must acknowledge the source in the figure captions.

9. References

- [1] Performance-based seismic fortification and design ground motion [M]. Beijing: Science press, 2009.
- [2] Singhal A, Kiremidjian A S. Method for probabilistic evaluation of seismic structural damage [J]. ASCE Journal of structural engineering, 1996, 122(12): 1459-1467.



- [3] Elnashai A S, Borzi B. Deformation-based vulnerability functions for RC bridges [J]. *Structural Engineering and Mechanics*, 2004, 17(2): 215-244.
- [4] Erberik MA, and Elnashai AS. Fragility analysis of flat-slab structures [J]. *Engineering Structures*, 2004, 26(7): 937-948.
- [5] Ji J, Elnashai AS, and Kuchma D. Seismic fragility relations of reinforced concrete high-rise buildings [J]. *The Structural Design of Tall and Special Buildings*, 2009, 18(3): 259-277.
- [6] Hwang H., Liu Jingbo. Vulnerability analysis of RC bridges under seismic ground motions [J]. *China Civil Engineering Journal*, 2004; 37(6): 47-51.
- [7] Hwang H, Liu J B, and Chiu Y H. Seismic fragility analysis of highway bridges [R]. Center for Earthquake Research and Information, the University of Memphis, 2001, Report.
- [8] Zhu Jian. Vulnerability analysis and seismic risk evaluation of RC structures [D]. Doctoral Dissertation, Xi'an University of Science and Technology, 2010.
- [9] Kinali K, Ellingwood B R. Seismic fragility assessment of steel frames for consequence-based engineering: A case study for Memphis, TN [J]. *Engineering Structures*, 2007, 29(6): 1115-1127.
- [10] Ellingwood B R, Celik O C, Kinali K. Fragility assessment of building structural systems in Mid-America [J]. *Earthquake Engineering and Structural Dynamics*, 2007, 36(13): 1935-1952.
- [11] Rosowsky D V, Ellingwood B R. Performance-based engineering of wood frame housing: fragility analysis methodology [J]. *ASCE Journal of Structural Engineering*, 2002, 128(1): 32-38.
- [12] Dimova S L, Negro P. Seismic assessment of an industrial frame structure designed according to Eurocodes. Part 2: capacity and vulnerability [J]. *Engineering Structures*. 2005, 27(5): 724-735.
- [13] Wang Dan. Seismic vulnerability analysis and probabilistic risk analysis of steel frame structures. [D]. Master's Dissertation, Harbin Institute of Technology, 2006.
- [14] Chang Zemin. Non-linear aseismic Reliability and seismic vulnerability Analysis of RC Structures [D]. Master's Dissertation, Harbin Institute of Technology, 2006.
- [15] LvDagang, Li Xiaopeng, Wang Guangyuan. Reliability and performance based seismic vulnerability analysis of overall structures [J]. *Journal of Natural Disasters*. 2006, 15(2): 107-114.
- [16] LvDagang, Wang Guangyuan. Reliability and sensitivity based seismic vulnerability analysis of partial structures [J]. *Journal of Natural Disasters*. 2006, 15(4): 157-162.
- [17] Huang Minggang. Seismic vulnerability, fatalness and risk analysis of RC continuous beam bridges [D]. Master's Dissertation, Harbin Institute of Technology, 2009.
- [18] Applied Technology Council, Federal Emergency Management Agency. Quantification of building seismic performance factors [R]. America: FEMA, 2008.
- [19] Zhang Lingxin, Jiang Jinren. Latin hypercube sampling application in reliability analysis of structures [J]. *World Earthquake Engineering*. 1997, 13(4): 1-6.
- [20] Shi Wei, Ye Lieping, Lu Xinzhen. Collapse resistant capacity study on RC frame structures under different seismic fortification levels [J]. *Engineering Mechanics*. 2011, 28(3): 41-48.
- [21] Scott H D, Park R, Priestly M J N. Stress-Strain Behavior of Concrete Confined by Overlapping Hoops at Low and High Strain Rates [J]. *Journal of the American Concrete Institute*. 1982, 79(1): 13-27.
- [22] Petrone C, Magliulo G, Giannetti L, et al. Stress-strain behavior of plasterboards subjected in tension and compression [C]// 16th World Conference on Earthquake Engineering, 2017.
- [23] ACT-63, Quantification of Building Seismic Performance Factors [S]. Applied Technology Council, 2010.
- [24] China National Standard: Code for Seismic Design of Buildings (GB50011-2010), (English), 2016.
- [25] Lucchini A, Franchin P, Mollaioli F. Generation of uniform hazard floor response spectra for linear MDOF structures [C]// 16th World Conference on Earthquake Engineering, 2017.